Differentiation of diastereomericN-aryltetrahydropyrano/tetrahydrofuranochromenylam under electron ionization and chemical ionization conditions

ARTICLE *in* RAPID COMMUNICATIONS IN MASS SPECTROMETRY · NOVEMBER 2007

Impact Factor: 2.25 · DOI: 10.1002/rcm.3239 · Source: PubMed

8 AUTHORS, INCLUDING:

Akkaladevi Venkatesham
Indian Institute of Chemical Technology
4 PUBLICATIONS **39** CITATIONS
SEE PROFILE

Kommu Nagaiah
Indian Institute of Chemical Technology
96 PUBLICATIONS **1,169** CITATIONS
SEE PROFILE

Ramisetti Nageswara Rao
Indian Institute of Chemical Technology
156 PUBLICATIONS **1,452** CITATIONS
SEE PROFILE

G Narahari Sastry
Indian Institute of Chemical Technology
262 PUBLICATIONS **5,205** CITATIONS
SEE PROFILE

RAPID COMMUNICATIONS IN MASS SPECTROMETRY
Rapid Commun. Mass Spectrom. 2007; **21**: 3511–3519
Published online in Wiley InterScience (www.interscience.wiley.com) DOI: 10.1002/rcm.3239

Differentiation of diastereomeric *N*-aryltetrahydropyrano/tetrahydrofuranochromenylamines under electron ionization and chemical ionization conditions†

G. S. Ramanjaneyulu[1], S. Prabhakar[1]*, G. Bhaskar[1], A. Venkatesham[2], K. Nagaiah[2], R. Nageswara Rao[3], Y. Soujanya[4] and G. Narahari Sastry[4]

[1]National Centre for Mass Spectrometry, Indian Institute of Chemical Technology, Hyderabad – 500 007, India
[2]Organic Chemistry Division, Fine Chemicals Laboratory, Indian Institute of Chemical Technology, Hyderabad – 500 007, India
[3]Analytical Chemistry Division, Indian Institute of Chemical Technology, Hyderabad – 500 007, India
[4]Molecular Modeling Group, Indian Institute of Chemical Technology, Hyderabad – 500 007, India

Received 28 May 2007; Revised 27 August 2007; Accepted 27 August 2007

A series of diastereomeric 4*S*,5*S*,6*R*/*S*-tetrahydropyrano- and 3*S*,4*S*,5*R*/*S*-tetrahydrofuranochromenylamine derivatives (a/b isomers; 1–26) has been studied under electron ionization (EI) and chemical ionization (CI) conditions. The EI mass spectra of all diastereomeric compounds show two characteristic fragment ions, of which one is formed by retro-Diels-Alder (RDA) reaction from the molecular ion, retaining the charge on the diene fragment, and the other $[M–(HNAr)]^+$ ion by a simple radical loss. The RDA process is more favorable in all b isomers, whereas the radical loss is dominant in all a isomers; based on these two ions it is easy to differentiate the two diastereomers. The collision-induced dissociation (CID) spectra of all the molecular ions also show the same trend, which reflects the stereoselectivity in the formation of the two characteristic fragment ions. The results of theoretical calculations performed are in accordance with the experimental observations. The CI experiments (methane and isobutane) on all the diastereomeric compounds also enabled the differentiation of the isomers. Copyright © 2007 John Wiley & Sons, Ltd.

Derivatives of pyran and fused 4*H*-pyran ring systems have different types of biological activity. This has attracted much interest towards the synthesis of 2*H*-1-benzopyrans (2*H*-chromenes) and 3,4-dihydro-2*H*-1-benzopyrans (chromans), which are representatives of naturally occurring bioactive compounds.[1] 4-Aminobenzopyrans and their derivatives have drawn considerable attention in the last decade as modulators of potassium channels influencing the activity of the heart and blood pressure. Fused tetrahydropyranobenzopyran and tetrahydrofuranobenzopyran derivatives are also frequently found in naturally occurring bioactive molecules, and this has led to the development of synthetic methods.[2] Yadav *et al*. reported a simple, one-pot synthesis of *N*-(aryl)-tetrahydropyranochromenylamines and *N*-(aryl)tetrahydrofuranochromenylamines by treating the appropriate salicylaldehyde Schiffs base with dihydropyran or dihydrofuran in the presence of a catalyst.[3] This reaction involves a Diels-Alder cycloaddition reaction and is expected to yield a mixture of stereoisomers, *viz*. the isomers due to ring fusion (*cis*/*trans* fusion) and the isomers due to generation of a new chiral center at the linkage of the *N*-aryl substituent. However, the experimental products are found to be exclusively the *cis*-fused linear tricyclic products; hence, there were only two diastereomers, differing at the stereochemistry of the *N*-aryl substituent. The diastereomeric *N*-(aryl) tetrahydrofuranochromenylamines can be easily separated by column chromatography, whereas diastereomeric *N*-(aryl)tetrahydropyranochromenylamines cannot be separated by column chromatography, but can be separated by gas chromatography (GC) or reversed-phase high-performance liquid chromatography (HPLC). Hyphenated techniques such as gas/liquid chromatography coupled to mass spectrometry (GC/MS or LC/MS), which enable simultaneous separation and identification, are ideal for the analysis of such reaction products, provided that the stereoisomers give distinct mass spectra. Therefore, knowledge of the mass spectral behavior of the diastereomeric tetrahydropyrano- or tetrahydrofuranobenzopyrans is crucial in the analysis of the above reaction mixtures.

Mass spectrometry is a proven technique for the differentiation of stereoisomers. The isomeric pyran derivatives have been studied by mass spectrometry[4] and the electron ionization (EI) fragmentations of pyran derivatives and their fused cyclic compounds have been documented.[5–7]

*Correspondence to: S. Prabhakar, National Centre for Mass Spectrometry, Indian Institute of Chemical Technology, Hyderabad – 500 007, India.
E-mail: prabhakar@iict.res.in
†IICT Communication number: 070415.

Fragmentations due to retro-Diels-Alder (RDA) reactions were found to be key to the characterization of these compounds. The RDA reaction has been successfully used to characterize different cyclic systems containing a double bond in a six-membered ring such as substituted cyclohexenes, tetralins,[8] fused bicyclic,[9,10] tricyclic,[11] polycyclic compounds,[12–14] oxazines,[15] isobenzofurans, naphthofurans,[16] isoquinolines,[17] chromans,[18,19] and chromones,[20] and also the differentiation of isomeric compounds.[21–24] RDA fragmentation has mainly been used to discriminate *cis*- and *trans*-fused cyclic compounds, wherein *cis*-fused isomers undergo RDA reaction more favorably than *trans*-fused isomers. To the best of our knowledge RDA fragmentation has rarely been used to distinguish the diastereomers which are due to a chiral center at a place other than the ring junctions of bicyclic/polycyclic compounds. Hence, we have undertaken the mass spectral study of the diastereomeric tetrahydropyrano/tetrahydrofuranobenzopyran derivatives under EI and chemical ionization (CI) conditions.

EXPERIMENTAL

Materials

The isomeric compounds **1–26** (Scheme 1, isomers **a** and **b**) were synthesized by the condensation of the appropriate salicylaldimine with dihydropyran or dihydrofuran in the presence of a catalyst using the procedure similar to that reported.[2,3] All the starting materials were purchased from Sigma-Aldrich (Steinheim, Germany), and the solvents for chromatographic and mass spectral analysis were purchased from Merck (Mumbai, India). The reaction products were separated by preparative HPLC (**7**, **8**, **15** and **16**) and column chromatography (**19–26**). The isolated compounds were characterized by the comparison of their NMR data with the reported NMR data.[2,3] These isomeric compounds also yielded distinct EI mass spectra. Since the other isomeric compounds (**1–6**, **9–14**, and **17–18**) were not separable by column chromatography, the reaction products were directly analyzed by GC/MS, where the two diastereomers were clearly separated. Here, the two isomers were characterized by their distinct EI mass spectra, and the observed spectral differences were similar to those found between the isolated diastereomeric compounds. In the diastereomeric pairs, the **a** isomers always elute faster than the **b** isomers in GC analysis (Scheme 1).

GC/MS analyses

All the GC/MS analyses were performed with an Agilent 6890 gas chromatograph (Agilent Technologies, Palo Alto, CA, USA) equipped with a model 5973N mass-selective detector. A HP-5 MS capillary column (length 30 m, 250 μm i.d. and 0.25 μm film thickness) was used and the column oven temperature program was 50°C (2 min), and then heated at 10°C/min to 280°C, where it was held for 3 min. Helium was used as the carrier gas at a flow rate of 1.0 mL/min. Typical EI conditions were: electron energy, 70 eV; ion source temperature, 230°C; interface temperature, 280°C; quadrupole analyzer temperature, 150°C. Typical CI (methane and isobutane) conditions were: electron energy, 100 eV (methane) or 175 eV (isobutane); source temperature, 180°C; quadrupole analyzer temperature, 106°C. The reagent gas pressures were maintained at a regulator pressure of 200–250 kPa with 10% and 20% of the total flow allowed into the ion source for methane/CI and isobutane/CI, respectively. The quadrupole analyzer was scanned over the range *m/z* 30–600 (EI) or 60–600 (CI) for all the GC/MS experiments.

The product/precursor ion spectra and high-resolution (HR) mass spectra of **1–8** and **11–18** were recorded using a

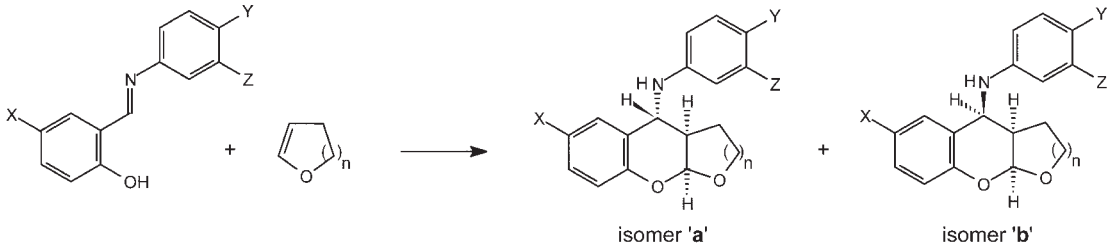

n = 2; N-Aryl tetrahydropyrano chromenyl amine

	4(S), 5(S), 6(R) - isomer	4(S), 5(S), 6(S) - isomer
X = H, Y= H, Z = H	**1**	**2**
X = Br, Y = H, Z= H	**3**	**4**
X = H, Y = CH_3, Z = H	**5**	**6**
X = H, Y = F, Z = H	**7**	**8**
X = H, Y = Cl, Z = H	**9**	**10**
X = H, Y = Z= F	**11**	**12**
X = Br, Y = B= Cl	**13**	**14**
X = H, Y = F, Z = Cl	**15**	**16**
X = H, Y = CH_3, Z = Cl	**17**	**18**

n = 1; N-Aryl tetrahydrofurano chromenyl amine

3(S), 4(S), 5(R) - isomer	3(S), 4(S), 5(S) - isomer
19	**20**
21	**22**
23	**24**
25	**26**

Scheme 1. Molecular structures of the studied isomeric compounds (**1–26**).

DOI: 10.1002/rcm

VG Autospec magnetic sector mass spectrometer (Waters, Manchester, UK). The collision-induced dissociation (CID) product ion spectra were measured using the linked-scan technique at constant B/E using nitrogen as the collision gas admitted into the first field-free region so that the main beam transmission was reduced to 30–40% of its original intensity. Precursor ion spectra were obtained using the linked scan at constant B^2/E. The HR mass spectral data were obtained at a resolution of 6000 (10% valley definition), unless otherwise stated, by voltage scan using perfluorotributylamine as the internal standard.

Computational details

All the structures, including reactants and all the possible products, were optimized using the B3LYP/6-31G (d) level, and the nature of the resultant stationary points was ascertained with frequency calculations. Geometry optimizations were carried out without any symmetry constraints. Vibrational frequencies were evaluated at the optimized geometries to verify the nature of the stationary points. The transition structures were characterized by one imaginary frequency and the intermediates, reactants and products all have real frequencies. Intrinsic reaction coordinate (IRC) calculations were performed in forward and backward directions, by following the eigenvector associated to the unique negative eigenvalue of the Hessian matrix to unambiguously establish the transition-state (TS) connectivity.

RESULTS AND DISCUSSION

Electron ionization

The isomeric compounds **1–26** are formed by the condensation reaction of an appropriate salicylaldimine with dihydropyran or dihydrofuran in the presence of an acid as a catalyst.[2,3] Since this condensation reaction is known to result in *cis*-fused furano/pyranobenzopyrans,[2,3] the reaction yielded two diastereomeric products because a new chiral center is generated at the carbon linked to the arylamine substituent (Scheme 1). For convenience, we denote the two diastereomeric products as **a** isomers [4*S*,5*S*,6*R*-isomer of *N*-(aryl)tetrahydropyranochromenylamines and 3*S*,4*S*,5*R*-isomer of *N*-(aryl)tetrahydrofuranochromenylamines] and **b** isomers [4*S*,5*S*,6*S*-isomer of *N*-(aryl)tetrahydropyranochromenylamines and 3*S*,4*S*,5*S*- isomer of *N*-(aryl)tetrahydrofuranochromenylamines] (Scheme 1). The EI mass spectra of all diastereomeric compounds (**1–26**) are summarized in Tables 1 and 2, and typical spectra of isomeric

Table 1. EI mass spectra of compounds **1–18**

	m/z (relative abundance, %)			
Compound No.	$M^{+\bullet}$	$[RDA]^{+\bullet}$	$[M–HNAr]^{+}$	Other ions
1	281 (47)	197 (100)	189 (89)	222(4), 208(3), 196(62), 158(3), 145(43),131(11), 107(10), 91(8), 77(28), 65(8), 55(7), 51(8)
2	281 (25)	197 (100)	189 (17)	196(51), 145(9), 91(3), 77(18), 65(3), 55(3), 51(4), 39(2)
3	359 (22)	275 (100)	267 (25)	274(25), 223(11), 195(4), 189(1), 188(8), 167(10), 145(7), 131(8), 119(1), 115(5), 102(4), 93(7), 77(24), 65(5), 55(4), 51(5), 39(3)
4	359 (19)	275 (100)	267 (8)	274(21), 223(3), 195(4), 188(3), 167(10), 145(3), 131(4), 119(1), 115(3), 102(2), 93(4), 55(3), 51(5), 39(2)
5	295 (70)	211 (91)	189 (100)	256(2), 210(58), 171(7), 161(8), 145(57), 133(10), 131(13), 118(7), 115(7), 107(52), 91(29), 77(13), 71(7), 65(12), 55(6), 51(4), 39(4)
6	295 (38)	211 (100)	189 (26)	256(1), 210(49), 171(2), 161(2), 145(17), 133(17), 131(6), 118(4), 115(3), 107(14), 91(18), 77(6), 65(7), 55(3), 51(2) 39(2)
7	299 (35)	215 (60)	189 (100)	215(60), 214(51), 171(5), 161(7), 145(43), 131(9), 122(7), 107(8), 95(14), 91(6), 77(7), 71(5), 65(4), 55(5), 39(3)
8	299 (30)	215 (100)	189 (32)	214(56), 171(2), 161(3), 145(15), 133(4), 122(6), 107(3), 95(11), 91(3), 77 (4), 65(2), 55(3), 39(2)
9	315 (26)	231 (38)	189 (100)	256(1), 230(29), 171(5), 167(4), 161(5), 145(40), 131(7), 120(4), 111(8), 107(6), 91(5), 77(5), 71(4), 65(3), 55(3), 39(2)
10	315 (31)	231 (100)	189 (52)	256(1), 230(49), 167(5) 145(22), 131(6), 120(6), 111(10), 107(4), 91(4), 77(5), 71(2), 65(2), 55(3), 51(2), 39(2)
11	317 (23)	233 (46)	189 (100)	232(34), 214(7), 203(3), 171(5), 161(6), 145(40), 133(8), 131(8), 120(9), 107(9), 91(6), 77(7), 55(6), 39(3)
12	317 (27)	233 (100)	189 (42)	232(46), 177(9), 161(6), 145(17), 131(10), 120(15), 91(7), 77(6), 55(8), 39(1)
13	427 (18)	343 (38)	267 (100)	342(5), 308(51), 266(7), 223(29), 209(6), 201(9), 187(10), 174(7), 160(15), 145(20), 144(6), 130(5), 102(6), 75(6), 71(5), 63(6), 55(6), 39(3)
14	427 (17)	343 (55)	267 (41)	342(6), 308(76), 266(11), 223(10), 209(5), 201(11), 187(10), 172(9), 160(7), 145(13), 130(4), 102(4), 75(6), 63(5), 55(6), 39(5)
15	333 (18)	249 (43)	189 (100)	248(30), 145(39), 130(10), 129(8), 120(6), 107(7), 91(5), 77(6), 55(4), 39(2)
16	333 (22)	249 (100)	189 (43)	248(45), 189(43), 145(8), 131(9), 129(9), 120(8), 107(4), 91(4), 77(5), 55(4), 39(2)
17	329 (26)	245 (23)	189 (100)	244(21), 228(4), 209(7), 152(10), 145(40), 131(7), 107(7), 89(6), 77(8), 55(3), 39(2)
18	329 (53)	245 (100)	189 (81)	244(68), 228(13), 209(17), 152(30), 145(35), 117(14), 89(12), 77(12), 55(5), 39(3)

DOI: 10.1002/rcm

Table 2. EI mass spectra of compounds **19–26**

	m/z (relative abundance, %)			
Compound No.	$M^{+\bullet}$	$[RDA]^{+\bullet}$	$[M\text{-}HNAr]^{+}$	Other ions
19	267 (35)	197 (60)	175 (100)	196(40), 167(4), 157(4), 147(14), 131(5), 115(5), 107(7), 91(8), 77(19), 65(11), 51(4), 39(3)
20	267 (27)	197 (100)	175 (33)	196(53), 147(6), 131(4), 120(5), 107(3), 104(4), 91(4), 77(16), 65(3), 51(4), 39(2)
21	281 (44)	211 (50)	175 (100)	210(32), 167(3), 157(5), 147(16), 131(6), 118(4), 107(25), 91(20), 77(7), 65(7), 51(2), 39(2)
22	281 (43)	211 (100)	175 (54)	210(54), 167(3), 157(3), 147(10), 131(6), 118(5), 107(13), 91(21), 77(6), 65(7), 51(2), 39(3)
23	285 (27)	211 (83)	175 (100)	214(79), 207(16), 192(17), 157(5), 147(15), 130(6), 115(4), 107(8), 91(9), 77(7), 65(5), 51(4), 41(3), 39(4)
24	285 (28)	215 (100)	175 (55)	214(69), 198(5), 185(6), 157(3), 147(9), 145(6), 131(5), 122(7), 120(7), 107(5), 95(14), 91(6), 77(4), 65(3), 51(3), 39(2)
25	301 (19)	231 (19)	175 (100)	281(8), 230(18), 207(14), 191(2), 167(3), 157(4), 147(13), 145(6), 131(5), 122(7), 115(4), 107(5), 91(6), 77(4), 65(3), 51(3), 39(2)
26	301 (35)	231 (86)	175 (100)	281(25), 267(5) 253(8), 230(48), 207(48), 191(2), 167(7), 157(4), 147(16), 131(9), 120(7), 111(12), 107(7), 91(7), 77(4), 65(3), 51(2), 39(2)

pairs of tetrahydropyranochromenylamines (**1** and **2**) and tetrahydrofuranochromenylamines (**19** and **20**) are given in Figs. 1 and 2, respectively. All spectra show abundant molecular ions (30–65%). The molecular ions with a methyl substituent on the *N*-aryl group or without any substituent (i.e. N-Ph) are found to be more abundant (more stable) than those with halogens as substituents on the *N*-aryl group. Similarly, among the **a** and **b** isomers, the relative abundance of molecular ions of **a** isomers decreased and that of the molecular ions of **b** isomers increased as the number and size of the halogen substituent increased on the *N*-aryl group. The general fragmentation pattern of **1–26**, based on precursor/product ion spectra and HR mass spectral data, is summarized in Scheme 2. The spectra include mainly two abundant fragment ions, of which one is due to the RDA reaction of the molecular ions retaining the charge on the diene fragment, i.e. substituted salicylaldimine. The other possible RDA product ions (*m/z* 84 for **1–18** and *m/z* 70 for **19–26**) are missing from the spectra perhaps due to the higher appearance energies of these species than of the RDA product ions observed in the spectra (Stevenson's rule[22,25]). The second abundant fragment ion in the spectra corresponds to the loss of the *N*-aryl substituent (HN•Ar) as a radical from the molecular ion by a simple homolytic cleavage of the C–N bond (Scheme 2). Apart from the above two dominant fragment ions, the spectra include other ions corresponding to $[RDA–H]^{+}$ formed via the $[RDA]^{+\bullet}$ by the loss of a hydrogen radical and the ion at *m/z* 145 formed by

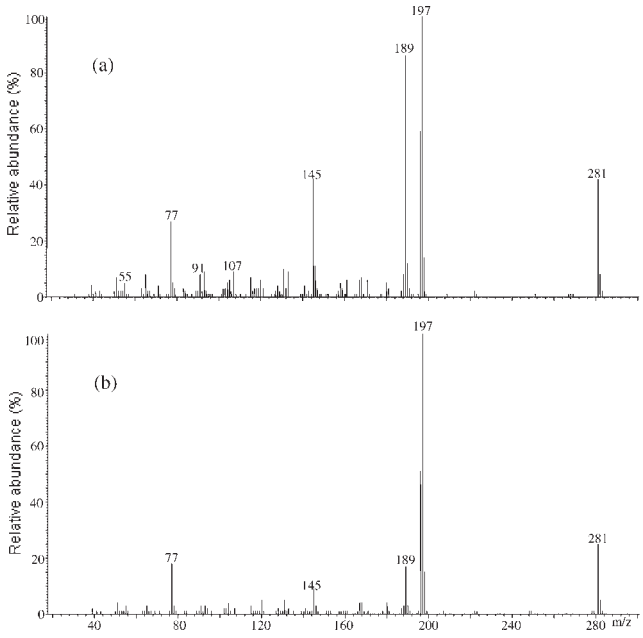

Figure 1. EI mass spectra of (a) compound **1** and (b) compound **2**.

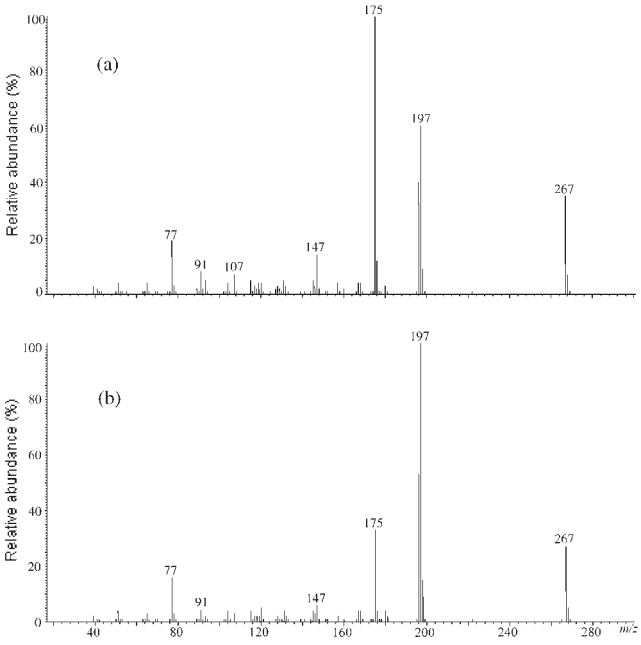

Figure 2. EI mass spectra of (a) compound **19** and (b) compound **20**.

DOI: 10.1002/rcm

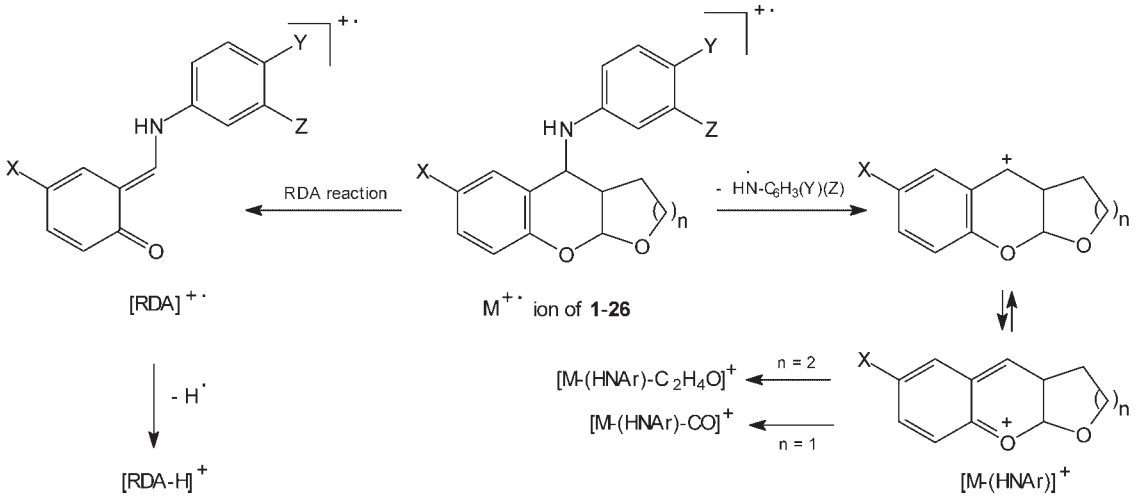

Scheme 2. EI fragmentation pattern of compounds **1**–**26**.

loss of C_2H_4O from the $[M–(HNAr)]^+$ ion (**1**–**18**) or *m/z* 147 due to CO loss from the $[M–(HNAr)]^+$ ion (**19**–**26**).

Although the isomeric compounds show the same three diagnostic fragment ions, namely $[M–(HNAr)]^+$, the RDA product ion and the ion at *m/z* 145/147, clear differences are observed in the relative abundances. The $[M–(HNAr)]^+$ ion is the base peak for the **a** isomers, and the RDA product ion is the base peak for the **b** isomers. Although the RDA fragment ion appears as the base peak in **1**–**4**, a clear-cut difference can be observed in the relative abundance of the $[M–(HNAr)]^+$ ion. Similarly, the spectra of the isomeric pair **25** and **26** exhibit the $[M–(HNAr)]^+$ ion as the base peak, but the difference in the relative abundance of the RDA fragment ion is significant. Therefore, formation of the $[M–(HNAr)]^+$ ion is feasible in all the **a** isomers, whereas the RDA reaction is favored in **b** isomers. As expected, the fragment ions due to further loss of C_2H_4O (**1**–**18**) or CO (**19**–**26**) from the $[M–(HNAr)]^+$ ion are always relatively more abundant for the **a** isomers than for the corresponding **b** isomers. Although the RDA fragment is diagnostic for the diastereomers, the differences in the relative abundances of $[RDA–H]^+$ are not as apparent as those of the $[RDA]^{+\cdot}$ ion. The observed differences between the spectra of diastereomeric pairs are still evident in the spectra recorded at low eV (15 eV). The spectra recorded at 15 eV look similar to those at 70 eV, except for a considerable reduction in the relative abundance of the $[RDA–H]^+$ ion with respect to that of the $[RDA]^{+\cdot}$ ion. We also conclude that there is no significant effect of source temperature on the spectra, because the spectra of isomeric compounds are similar at different source temperatures (120, 150, 180, 200 and 230°C).

We have also attempted to check the effect of the substituent located at the *para* position of the aryl group in the yields of the two diagnostic fragment ions. For this purpose, the percentages of total ionization (%TIC) of the $[M–(HNAr)]^+$ and $[RDA]^{+\cdot}$ ions were calculated. Among the **a** isomers, the %TIC of the $[M–(HNAr)]^+$ ion is increased for the Cl substituent (**9**, **13**, **15** and **17**) compared with the hydrogen or methyl substituent (**1** and **5**); the %TICs of the $[M–(HNAr)]^+$ ion are 20, 18, 34, 29, 36 and 38 in **1**, **5**, **9**, **13**, **15** and **17**, respectively. When the substituent was F the %TIC of the $[M–(HNAr)]^+$ ion increased (27 in **7**) but not to the extent observed with Cl. This difference in the formation of the $[M–(HNAr)]^+$ ion could be explained by the different stabilities of the leaving radicals (H·N-Ar radical). The H·N-C_6H_4-Cl radical is more stable than the H·N-C_6H_4-X radical (where X = F, H or CH_3) because of the mesomeric (+M) effect of chlorine. Similarly, among the **b** isomers, the %TIC of the $[RDA]^{+\cdot}$ ion decreased (43, 33, 32, 19, and 22 in **2**, **6**, **10**, **14** and **18**, respectively) with Cl substituents with an intermediate effect for the F substituent. Although the formation of the $[RDA]^{+\cdot}$ or $[M–(HNAr)]^+$ ions shows substituent effects, no significant effect can be found in the overall discrimination between the **a** and **b** isomers.

We also carried out CID experiments on the molecular ions to study whether the stereoselectivity in the formation of characteristic fragment ions is maintained in the dissociation of molecular ions. The CID spectra of all the molecular ions are very clear and include mainly two characteristic ions corresponding to $[M–(HNAr)]^+$ and $[RDA]^{+\cdot}$. Typical molecular ion CID spectra obtained from **17** and **18** are shown in Fig. 3. As observed in the EI spectra, the CID spectra of all the **a** isomers show a dominant $[M–radical]^+$ ion, whereas the spectra of the corresponding **b** isomers show a dominant $[RDA]^{+\cdot}$ ion. The CID spectra of **1**–**4** show the RDA product ion as the major ion; however, the abundance of the $[M–(HNAr)]^+$ ion is relatively higher in **1** and **3** (**a** isomers) than in the corresponding isomers **2** and **4** (**b** isomers), and this is similar to the trend observed in the EI spectra.

In solution, the Diels-Alder reactions yield *endo*-isomers (stable kinetically, but not thermodynamically) as major products because the *endo* transition state is stabilized by secondary interactions; and the *exo*-isomers are always minor products. The thermodynamic instability of the product leads to a backward reaction when it is given high energy. In the present study, the RDA fragmentation is always dominant in **b** isomers (like *endo*-isomers) compared with **a** isomers, which suggests that the **b** isomers must be highly energetic compared with the **a** isomers and hence undergo RDA fragmentation due to their thermodynamic instability. We have performed theoretical calculations on the molecular

DOI: 10.1002/rcm

RCM

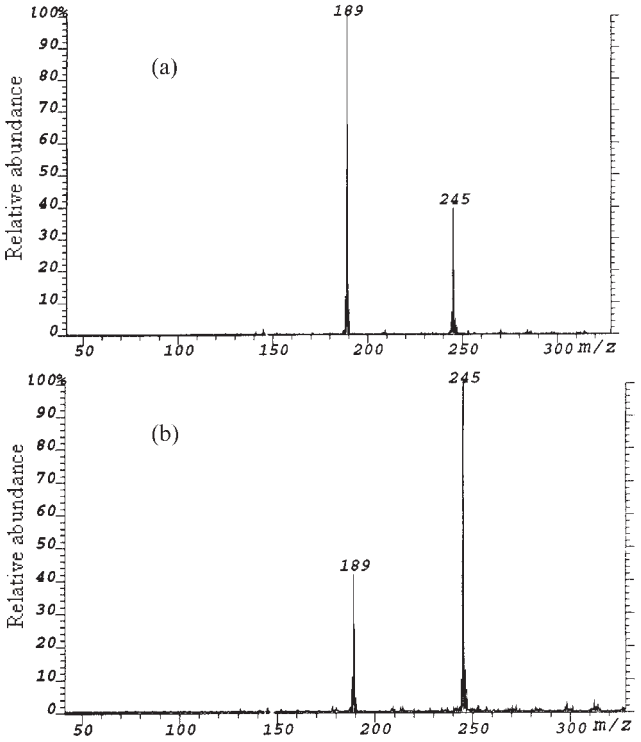

Figure 3. CID spectra of $M^{+\bullet}$ of (a) compound **17** and (b) compound **18**.

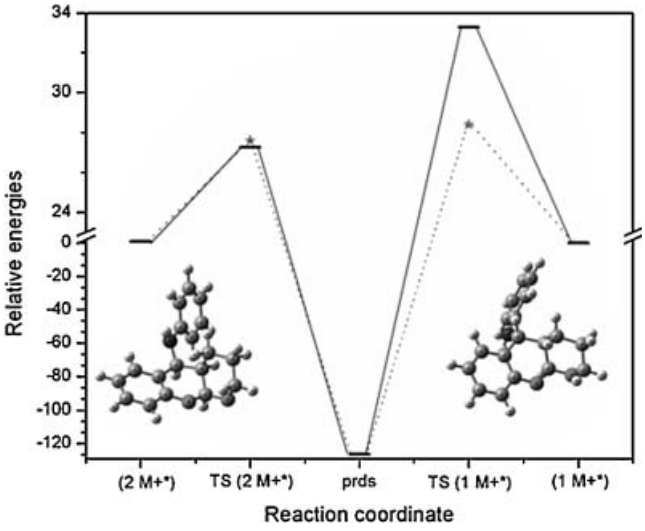

Figure 4. Reaction profile for reactants, transition states (RDA and radical loss) and products of isomer **1**$M^{+\bullet}$ and **2**$M^{+\bullet}$ obtained at B3LYP/6-31G*. (★) indicates the transition states for the loss of radical from molecular ion and (—) indicates the transition state for the RDA reaction.

ions of **1** and **2** to calculate the internal energy of the isomers (Table 3) and the internal energy of the **b** isomer (**2**) is indeed more than that of the corresponding **a** isomer (**1**). Moreover, the transition-state (TS) energies were calculated for the RDA fragmentation reaction, and proved that RDA fragmentation is feasible for the **b** isomers (**2**, Fig. 4), the potential energy barrier for which is low, whereas for the **a** isomers (**1**, Fig. 4) this reaction is difficult because the transition state requires very high energy. We have also calculated the TS energies for the radical loss reaction from the molecular ions of **1** and **2**. The TS energy of radical loss from the molecular ion of **2** is very close (slightly higher) to that of the RDA reaction; hence both ions are abundant in **2**. However, the TS energy of radical loss from the molecular ion of **1** is very much lower than that of the RDA reaction; hence radical loss is favored in **1** compared with the RDA reaction, which is highly energetic.

Chemical ionization

We extended the study under CI conditions using isobutane and methane as the reagent gases to check whether the stereoselectivity observed in the fragmentation of molecular ions is maintained in protonated molecules, $[M+H]^+$ ions. Isobutane/CI spectra of all the compounds show abundant $[M+H]^+$ ions (10–100%) in addition to a weak $M^{+\bullet}$ (relative abundance (RA) <10%) ion and the characteristic adduct ions $[M+43]^+$ and $[M+57]^+$. The isobutane/CI spectra of **1–26** are summarized in Table 4, and the CI spectra of **7** and **8** are given in Fig. 5 as examples. The general fragmentation pattern observed under CI conditions is shown in Scheme 3. The fragment ion due to the RDA reaction, $[diene+H]^+$, is also observed under CI conditions; RDA fragmentation under CI conditions is a well-known process.[13,14,22] Interestingly, low abundance $[diene+C_3H_7]^+$ and $[diene+C_4H_9]^+$ ions were also detected and they might result from the RDA reaction of the $[M+43]^+$ and $[M+57]^+$ ions. The spectra also include $[M+H–C_6H_5OH]^+$ and $[X–C_6H_4–NH_3]^+$ ions at varied relative abundances. Among diastereomeric pairs, the relative abundance of the $[M+H]^+$ ion is consistently higher for the **a** isomers than for the **b** isomers, whereas the relative abundance of the RDA product ion is relatively higher for the **b** than for the **a** isomers. The %TICs for all the ions in the spectra were also calculated to check the significance of the $[MH–NH_2Ar]^+$ ion, and it was found that formation of this ion is relatively more favored for the **b** than for the **a** isomers. The %TICs of the $[M+H]^+$ and RDA

Table 3. Ground-state energies for molecular ions of **1** and **2** and transition-state energies for RDA/radical loss processes obtained from theoretical calculations

Structure	Ground-state energy (a.u.)	Relative energy[a] (kcal/mol)	TS energy of RDA reaction (a.u.)	Reaction energy barrier for RDA reaction (kcal/mol)	TS energy for radical loss (a.u.)	Reaction energy barrier for radical loss (kcal/mol)
2$M^{+\bullet}$	−902.30237	0.92	−902.25894	27.26	−902.25838	27.61
1$M^{+\bullet}$	−902.30384	0.00	−902.25080	33.28	−902.25855	28.42

[a] Relative energy with respect to the most stable structure.

DOI: 10.1002/rcm

Table 4. Isobutane/CI mass spectra of **1–26**

	m/z (relative abundance, %)			
Compound No.	$[M+H]^+$	$[RDA]^+$	$[MH–H_2NAr]^+$	Other ions
1	282 (74)	198 (21)	189 (100)	338(7), 324(3), 281(12), 254(2), 245(2), 240(2), 231(1), 94(18)
2	282 (52)	198 (40)	189 (100)	338(11), 324(4), 281(16), 254(9), 245(3), 240(4), 231(1), 94(8)
3	360 (72)	276 (16)	267 (100)	416(4), 402(4), 359(12), 334(3), 318(4), 189(9), 150(5), 132(5), 94(55)
4	360 (81)	276 (27)	267 (100)	416(10), 402(6), 359(18), 332(6), 318(4), 189(8), 150(2), 132(4), 94(16)
5	296 (100)	212 (19)	189 (79)	352(6), 338(3), 295(22), 268(4), 254(4), 212(19), 202(6), 164(2), 146(3), 108(3)
6	296 (95)	212 (46)	189 (100)	352(6), 338(5), 295(34), 268(10), 254(6), 212(46), 202(3), 164(1), 146(2), 108(2)
7	300 (54)	216 (16)	189 (100)	356(3), 342(2), 299(12), 272(3), 258(2), 245(2), 231(1), 216(16), 206(5), 112(8)
8	300 (33)	216 (33)	189 (100)	356(6), 342(5), 299(17), 272(9), 258(4), 245(4), 231(1), 216(33), 206(2), 112(3)
9	316 (41)	232 (12)	189 (100)	372(2), 358(4), 315(10), 296(4), 274(2), 232(12), 222(4), 145(1), 128(4), 245(2)
10	316 (20)	232 (24)	189 (100)	372(6), 358(5), 315(10), 288(8), 274(2), 232(24), 222(1), 128(3), 245(1)
11	318 (39)	234 (20)	189 (100)	374(1), 360(1), 317(10), 290(4), 276(3), 234(20), 130(5)
12	318 (11)	234 (34)	189 (100)	374(1), 360(2), 317(10), 290(8), 276(2), 245(3), 234(34), 130(8)
13	428 (14)	344 (8)	267 (100)	484(1), 470(2), 427(7), 400(2), 386(4), 344(6), 314(11), 189(6), 162(2)
14	428 (8)	344 (8)	267 (100)	484(1), 470(2), 427(7), 400(2), 392(6), 386(2), 344(8), 314(6), 189(2), 162(1)
15	334 (39)	250 (15)	189 (100)	390(1), 376(1), 333(8), 306(2), 292(2), 250(15), 245(2), 240(2), 231(1), 146(10)
16	334 (16)	250 (29)	189 (100)	390(5), 376(6), 333(10), 306(8), 292(3), 250(29), 146(4)
17	330 (60)	246 (15)	189 (100)	386(6), 372(3), 329(10), 302(2), 288(2), 246(15), 142(10)
18	330 (44)	246 (29)	189 (100)	386(11), 372(5), 329(11), 302(7), 288(2), 246(29), 142(14)
19	268 (100)	198 (29)	175 (85)	324(6), 310(4), 267(16), 254(3), 240(3), 94(10)
20	268 (44)	198 (41)	175 (100)	324(7), 310(4), 267(16), 254(8), 240(4), 94(7)
21	282 (100)	212 (25)	175 (57)	338(6), 324(4), 281(18), 268(4), 254(4), 108(10)
22	282 (73)	212 (55)	175 (100)	338(6), 324(4), 281(19), 268(10), 254(4), 231(1), 108(29)
23	286 (63)	216 (28)	175 (100)	342(3), 324(1), 285(12), 272(5), 258(4), 231(4), 192(5), 112(45)
24	286 (23)	216 (36)	175 (100)	342(4), 328(4), 285(12), 272(9), 258(3), 231(2), 192(5), 112(16)
25	302 (40)	232 (17)	175 (100)	358(2), 344(2), 301(9), 288(3), 274(2), 208(4), 128(25)
26	302 (16)	232 (29)	175 (100)	358(3), 344(4), 301(9), 288(6), 274(2), 128(25)

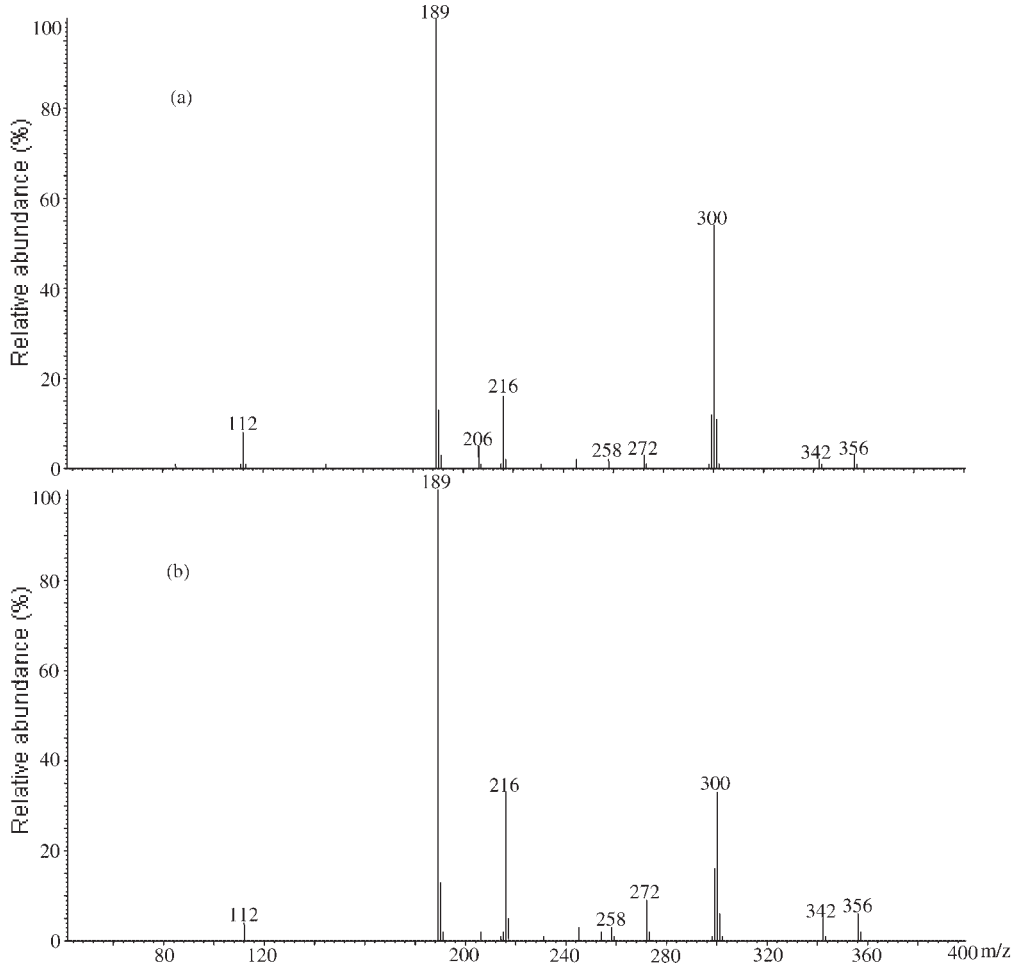

Figure 5. Isobutane/CI mass spectra of (a) compound **7** and (b) compound **8**.

DOI: 10.1002/rcm

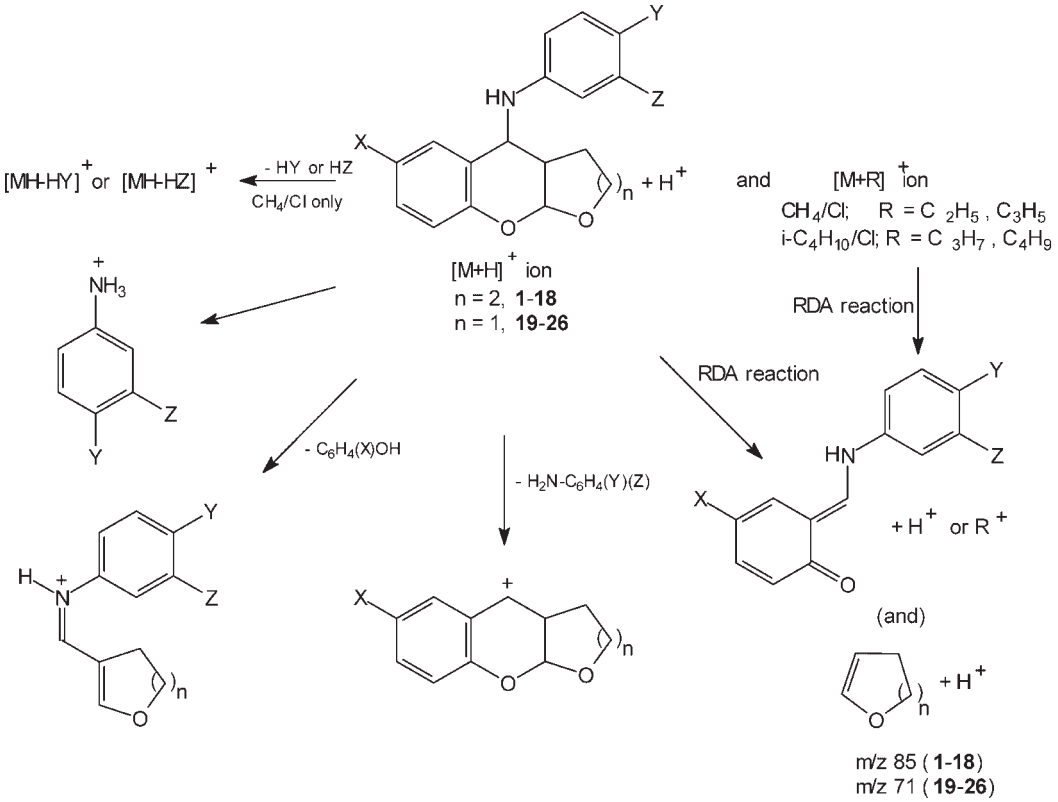

Scheme 3. CI fragmentation pattern of compounds **1**–**26**.

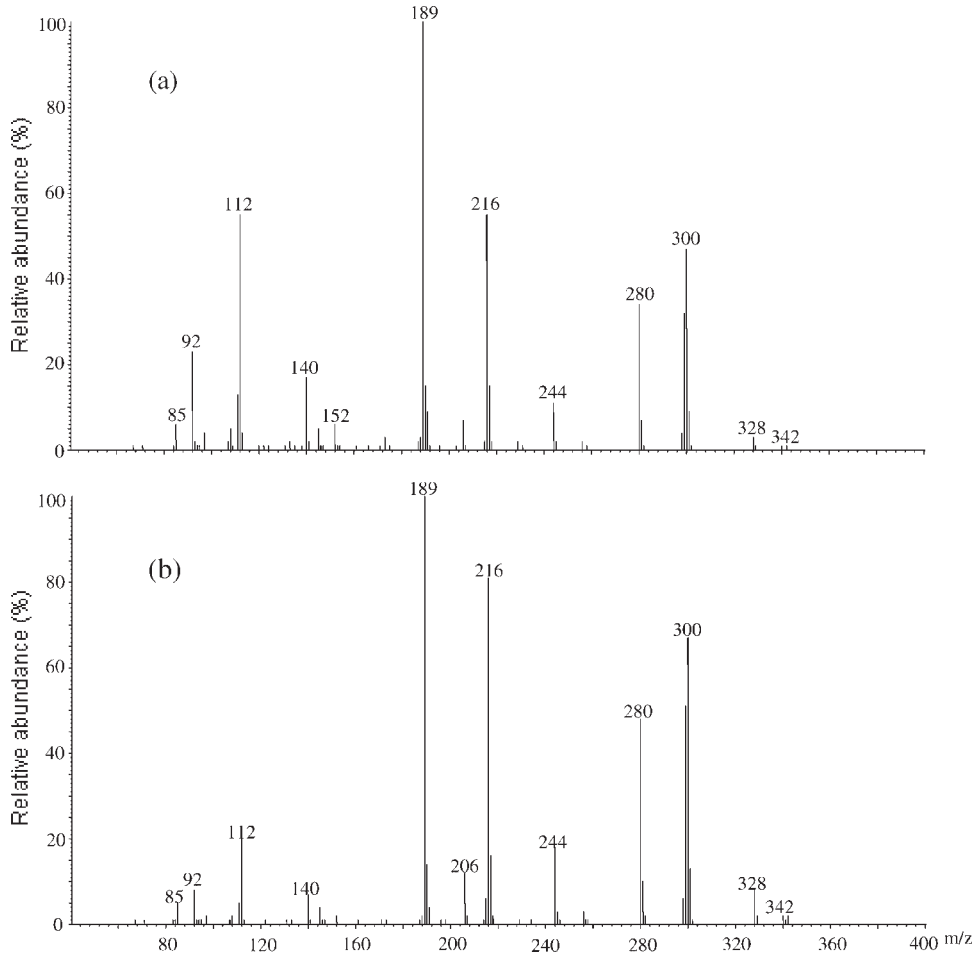

Figure 6. Methane/CI mass spectra of compounds (a) **7** and (b) **8**.

DOI: 10.1002/rcm

product ions show a similar trend to that observed in their relative abundances.

The methane/CI spectra of **1**–**26** consist of almost the same fragment ions as found in the isobutane/CI spectra (Scheme 3) but, as expected, the abundances of fragment ions are higher. Typical methane/CI spectra of **7** and **8** are given in Fig. 6. All the spectra show fragment ions due to the RDA reaction, i.e. $[diene+H]^+$ and protonated dihydropyran/dihydrofuran including $[diene+C_2H_5]^+$ and $[diene+C_3H_5]^+$ ions from $[M+29]^+$ and $[M+41]^+$ ions, respectively (data not shown). Whenever there are F or Cl substituents on the *N*-aryl group, an additional loss of HF and HCl is observed. Formation of the $[X–C_6H_4–NH_3]^+$ ions is found to be characteristic for the **a** isomers, being consistently more abundant than for the **b** isomers. All other fragment ions are found to be relatively higher for the **b** than for the **a** isomers. However, the spectral differences between the isomeric compounds are not as apparent in the methane/CI spectra as in the isobutane/CI spectra.

CONCLUSIONS

The present mass spectral study on isomeric tetrahydropyrano/tetrahydrofuranochromenylamines (isomers **a** and **b**; **1**–**26**) shows that the isomers could be differentiated by their stereoselective RDA reaction. Under EI conditions, the relative abundance of the RDA fragment ion is greater in **b** isomers, whereas the fragment ion due to simple radical loss, the $[M-(HNAr)]^+$ ion, is dominant in **a** isomers. The selectivity in the formation of these two characteristic fragment ions is more prominent when electron-withdrawing Cl is present on the aryl group attached to nitrogen. Theoretical calculations reveal a higher potential energy barrier for the RDA reaction in the **a** than in the **b** isomers; hence the RDA product ion is dominant in the **b** isomers. The isobutane/CI experiments reflect the same stereoselectivity. Methane/CI spectra also show characteristic fragment ions enabling differentiation of the isomers; the $[X–C_6H_4–NH_3]^+$ ion is found to be consistently more abundant for the **a** than for the **b** isomers.

Acknowledgements

The authors thank Dr J. S. Yadav, Director, IICT, for facilities and encouragement, and Dr. M. Vairamani for guidance and support. GSR thanks CSIR, New Dehli, and GB and AV thank UGC, New Delhi, for the senior research fellowships.

REFERENCES

1. Abdel-Waheb AHF. *Acta. Pharm.* 2002; **52**: 269.
2. Anniyappan M, Muralidharan D, Perumal PT. *Tetrahedron* 2002; **58**: 10301.
3. Yadav JS, Reddy BVS, Madhuri Ch, Sabitha G, Jagannadh B, Kumar SK, Kunwar AC. *Tetrahedron Lett.* 2001; **42**: 6381.
4. Bravo P, Ticozzi C, Daolio S, Traldi P. *Org. Mass Spectrom.* 1985; **20**: 740.
5. De Lucas A, Fernandez-Gadea J, Martin N, Martinez R, Seoane C. *Rapid Commun. Mass Spectrom.* 2000; **14**: 1783.
6. Morizur JP, Mercier J, Saraf M. *Org. Mass Spectrom.* 1982; **17**: 327.
7. Szmigielski R, Danikiewicz W, Dolatowska K, Wojciechowski K. *Int. J. Mass Spectrom.* 2006; **248**: 148.
8. Budzikiewicz H, Brauman JI, Djerassi C. *Tetrahedron* 1965; **21**: 1885.
9. Bohlmann F, Fischer CH, Forster J, Mathar W, Schwarz H. *Org. Mass Spectrom.* 1975; **10**: 1141.
10. Pihlaja K, Himottu M, Ovcharenko V, Frimpong-Manso S, Stajer G. *Rapid Commun. Mass Spectrom.* 1997; **11**: 249.
11. Bel P, Mandelbaum A. *Org. Mass Spectrom.* 1981; **16**: 513.
12. Lesman T, Deutsch J. *Org. Mass Spectrom.* 1973; **7**: 1321.
13. Etinger A, Mandelbaum A. *Org. Mass Spectrom.* 1992; **27**: 761.
14. Burinsky DJ, Dunphy R, Alvessantana JD, Cotter ML. *Org. Mass Spectrom.* 1991; **26**: 669.
15. Pihlaja K, Ovcharenko VV, Stajer G. *J. Am. Soc. Mass Spectrom.* 1999; **10**: 393.
16. Dibble PW, Rodrigo R. *Org. Mass. Spectrom.* 1988; **23**: 743.
17. Ibanez AF, Iglesias GYM. *Org. Mass Spectrom.* 1991; **26**: 132.
18. Eguchi S. *Org. Mass Spectrom.* 1978; **13**: 653.
19. Eguchi S. *Org. Mass Spectrom.* 1979; **14**: 345.
20. Martin N, Martinez-Alvarez R, Seoane C, Suarez M, Salfran E, Verdecia Y, Sayadi NK. *Rapid Commun. Mass Spectrom.* 2001; **15**: 20.
21. Morlender-vais N, Mandelbaum A. *J. Mass Spectrom.* 1998; **33**: 229.
22. Zitrin S, Yinon J, Mandelbaum A. *Tetrahedron* 1978; **34**: 1199.
23. Das KG, Madhusudanan KP. *Org. Mass Spectrom.* 1973; **7**: 619.
24. Maccioni AM, Traldi P. *J. Heterocycl. Chem.* 1987; **24**: 895.
25. Audier HE. *Org. Mass Spectrom.* 1969; **2**: 283.

DOI: 10.1002/rcm